Civil Engineering Infrastructures Journal, 2026, 59(1): 241-253
DOI: 10.22059/ceij.2024.369661.1996

TECHNICAL NOTE

Thermal Performance Prediction for Alkali-Activated Concrete Using GGBFS, NaOH and Sodium Silicate

Kumar, P.[1], Sharma, S.[2], Kumar, P.S.[1], Yuvaraj, M.S.[1], Purushotham, D.V.[1], Kumar, S.[3], Vashistha, K.K.[3], Kumar, A.[3*] and Gogineni, A.[2]

[1] Assistant Professor, Department of Civil Engineering, Mohan Babu University (SVEC), Tirupati, Andhra Pradesh, India.
[2] Research Scholar, Department of Civil Engineering, National Institute of Technology, Jamshedpur, Jharkhand, India.
[3] Assistant Professor, Department of Civil Engineering, IIMT University, Meerut, Uttar Pradesh, India.

Received: 15 Dec. 2023; Revised: 28 Aug. 2024; Accepted: 1 Sep. 2024

ABSTRACT: In fire safety, understanding the behaviour of concrete exposed to high temperatures is essential. This study experimentally explored the mechanical properties of Alkali-Activated Concrete (AAC) and utilized Recurrent Neural Network (RNN)-based Long Short-Term Memory (LSTM) techniques to predict the mechanical properties of AAC at elevated temperatures. The LSTM models accurately predicted compressive, flexural, and split tensile strengths, with coefficients of determination (R^2) exceeding 0.9 for training and testing datasets. Specifically, R^2 values were 0.9838 and 0.9134 for compressive strength, 0.9965 and 0.9861 for flexural strength, and 0.9743 and 0.9852 for split tensile strength in training and testing, respectively. The models also yielded low Root Mean Square Error (RMSE) and Mean Absolute Error (MAE) values, further underscoring their predictive reliability. Error analysis across all mechanical properties affirmed the LSTM models' robustness in capturing AAC's complex behaviour under thermal stress. These results suggest that LSTM networks are highly effective tools for predicting material properties crucial for structural fire safety and sustainable construction, offering a promising approach for improving the resilience and safety of AAC structures in extreme conditions.

Keywords: Alkali-Activated Concrete, Elevated Temperature, LSTM, Mechanical Properties, Prediction of Strengths.

1. Introduction

In 2014, Thailand's cement production industry significantly released carbon dioxide (CO_2) and other greenhouse gases into the atmosphere. The country's cement production emissions amounted to 36.92 tons per year, accounting for approximately 15% of Thailand's total CO_2 emissions. It is well known that greenhouse gas emissions tend to increase in proportion to the output of cement manufacturing (Zakka et al., 2021). Cement production involves a highly energy-intensive process that requires raising the temperatures of the raw materials to around 1400 °C (Dueramae et al., 2020; Gogineni et al., 2024a; Mishra et al., 2024). This energy input contributes to

* Corresponding author E-mail: amitsanajsr93@gmail.com

the overall carbon footprint of the cement industry. As a result, researchers have been exploring alternative approaches to reduce the environmental impact of cement production (Patel and Shah, 2018). One focus area has been replacing Ordinary Portland Cement (OPC) with supplementary cementing materials.

Numerous pozzolanic materials have been studied as potential replacements for OPC, including fly ash, bottom ash, palm oil fuel ash, rice husk ash, and bagasse ash. Fly ash has emerged as a promising candidate for widespread cement replacement in concrete due to its beneficial properties as a pozzolanic material (Namarak et al., 2018). Recently, alkaline cement, also known as geopolymers, has gained significant attention as an alternative to Portland cement-based concrete (Duxson et al., 2007). This is due to their distinctive qualities, which include rapid growth of high mechanical strength, and outstanding durability.

Unlike Portland cement, which exhibits low thermal conductivity and is non-combustible, sustained exposure to fire can lead to severe spalling, structural damage, or even collapse, posing risks to human life and resulting in high economic costs (Mostafaei et al., 2022). The behavior of Portland cement-based concrete under fire conditions can be attributed to the role played by Portland cement paste. When subjected to temperatures of around 95 ^{o}C, the primary binder in Portland cement, known as C-S-H gel, undergoes dehydration and significant shrinkage (Pratap and Kumar, 2024). Simultaneously, tiny explosions occur within the material.

At higher temperatures, such as 450 ^{o}C, portlandite decomposes; 750 ^{o}C calcium carbonate decomposes. Rehydration of the cement upon contact with water leads to its disintegration (Neville, 1995). In contrast, alkaline cement or geopolymers are based on a new family of aluminosilicate binders.

These materials, such as metakaolin or fly ash, undergo hydration in alkalis, forming a three-dimensional alkaline aluminosilicate hydrate known as N-A-S-H gel. This gel differs from the C-S-H gel formed during Portland cement hydration (Garcia-Lodeiro et al., 2011). Additionally, secondary reaction products in alkaline cement include various zeolites, such as hydroxy-sodalite, Na-chabazite, and zeolite. The specific zeolites that form depend on the alkaline activator and curing conditions (Kovalchuk et al., 2007; Criado et al., 2010). One of the most significant advantages of alkaline cement is its ability to develop high mechanical strength within a short period, even at moderate temperatures below 100 ^{o}C (Fernandez-Jimenez et al., 2006). This rapid strength development is beneficial in construction projects where early strength gain is desired. Moreover, alkaline cements exhibit excellent durability (Chithambaram et al., 2019; Singh et al., 2024; Mostafaei et al., 2023), making them suitable for applications that require long-lasting and resilient materials.

The key defining properties of alkaline cement are its rapid strength development and durability (Abhishek et al., 2022; Reddy and Harihanandh, 2023). Rapidly achieving high mechanical strength enables more rapid construction and shorter project schedules. The durability of alkaline cement ensures that structures built with these materials can withstand environmental factors and ageing processes, leading to longer service life and reduced maintenance costs. Alkali-Activated Concrete (AAC) has gained attention as a sustainable and eco-friendly alternative to traditional cement-based concrete. AAC offers several advantages, including lower power consumption and reduced greenhouse gas emissions while maintaining excellent mechanical and durability properties. AAC is a concrete type formed through polymerization or alkali activation. This process involves using alkaline activators to react with silica (Si), alumina (Al), and calcium (Ca) rich precursors, resulting in the formation of amorphous or semi-crystalline three-

dimensional alumino-silicates known as geopolymer or AAC.

Previous studies have shown that AAC systems have the potential to significantly reduce CO_2 emissions and energy demand compared to ordinary Portland cement (Mostafaei et al., 2023; Gogineni et al., 2024a). It is estimated that AAC can achieve more than a 50% reduction in CO_2 emissions and a 50-65% decrease in energy demand (Shah et al., 2020; Alrefaei and Dai, 2018). In addition to its excellent working properties and environmental benefits, AAC stands out because it predominantly utilizes industrial waste materials as its source material. This approach reduces the reliance on non-renewable raw materials and promotes the beneficial utilization of industrial waste.

Industrial wastes such as fly ash and slag are commonly used in AAC production due to their cost-effectiveness (Duxson et al., 2007), widespread availability (Xu et al., 2014), and sustainability. Fly ash, a by-product of coal combustion, is rich in silica and alumina (Paswan et al., 2024). It contributes to the final AAC product's stability, strength, and durability. However, fly ash exhibits low reactivity at room temperature. On the other hand, slag, a by-product of metal smelting, is rich in calcium and alumina. It offers higher strength but may have drawbacks such as longer setting time, poor workability, and sometimes lower durability and stability (Shah et al., 2020; Sharma et al., 2024). To optimize the properties of AAC, a combination of fly ash and slag, or a mixture of these materials with similar substances, is often employed.

This combination creates a stable final product with high strength and durability characteristics. Developing an AAC with similar strength properties to conventional AAC has simplified its application in in-situ scenarios. This advancement allows for the use of solid alkali, making it more convenient for on-site construction. However, achieving the desired fresh properties, satisfactory strength characteristics, and the proclaimed environmental benefits of AAC can be a complex process due to the nature and diversity of available source materials.

Designing an AAC mix requires carefully selecting input materials and their proportions, which typically involves extensive experimentation. This process demands significant amounts of material, time, and labour. Soft computing techniques and machine learning models have become imperative to overcome these challenges and streamline the AAC design process. By employing machine learning models (Gogineni et al., 2024b; Pratap et al., 2024), researchers can swiftly and efficiently predict the working properties of AAC. These computational tools can analyse large amounts of data, identify patterns, and generate predictive models that assist in selecting the optimal mix proportions for AAC production. This approach saves time, reduces material waste, and enhances the overall efficiency of AAC development, enabling faster adoption of this eco-friendly construction material. Since the early 2000s, neural networks (Zurada, 1992) have emerged as powerful and widely used tools for creating predictive models in concrete technology.

Machine Learning (ML) models (Gogineni et al., 2023a; Kumar et al., 2025b) revolutionize how predictions and decisions are made by leveraging mathematical models derived from sample data, eliminating the need for explicit programming. This paradigm shift allows for the development of sophisticated models capable of predicting diverse outcomes.

Concrete strength prediction is a prime example of how ML techniques, including neural networks, Support Vector Regression (SVR), and tree-based models, have been employed to enhance accuracy and efficiency. In a study by Huynh et al. (2020), the application of artificial intelligence was extended to predicting the compressive strength of fly ash-based geopolymer concrete. The researchers explored various ML models (Kumar et al.,

2023; Gogineni et al., 2026), including ANN (Kumar and Pratap, 2023), Deep Neural Networks (DNN), and Deep Residual Networks (ResNet) (Lieu et al., 2022; Lee et al., 2021). These models, particularly DNN and ResNet, demonstrated their prowess in capturing complex patterns within the data, thereby improving the accuracy of concrete strength predictions.

Another noteworthy approach involves the utilization of the Extreme Learning Machine (ELM) and ANN (Kim and Kim, 2002) for predicting the compressive strength of concrete containing fly ash and silica fume. The comparison of these models provides insights into their respective strengths and weaknesses, aiding researchers and practitioners in selecting the most suitable model for specific applications. Bai et al. (2003) utilized ANNs to predict the workability of concrete by incorporating various alumino-silicate by-product materials like metakaolin and fly ash. Recognizing the strong correlation between mix-design factors and the strength parameters of concrete composites, Yang et al. (2003) and Jithendra and Elavenil (2020) utilized ANNs to analyze these correlations.

The neural network later found applications in a variety of concrete composites, including self-compacting concrete (Kumar et al., 2025a), high-strength concrete (Khosravani et al., 2019), fiber-reinforced concrete (Liu and Zhang, 2020), and Geopolymer concrete (Nagajothi and Elavenil, 2020). According to the literature, neural network has been proven to be a highly effective technique for forecasting various concrete composite characteristics and other material investigations (Nagaraj et al., 2021; Kumar et al., 2024; Gogineni et al., 2024b). The AAC has superior durability and environmental benefits to traditional Portland cement concrete. However, accurately predicting its mechanical properties, such as compressive strength, flexural strength, and split tensile strength, particularly at elevated temperatures, remains challenging.

Traditional methods often fail to provide precise predictions due to the complex behavior of AAC under varying conditions. The present study addresses this challenge by predicting AAC properties at ambient and elevated temperatures using advanced soft computing techniques, specifically Long Short-Term Memory (LSTM) networks. LSTM, an advanced variant of fundamental algorithms like ANN and Recurrent Neural Networks (RNN), is designed to handle time-series data and capture long-term dependencies effectively. The present seeks to offer an efficient and accurate method for predicting the mechanical properties of AAC, addressing a significant gap in the existing literature where limited studies have focused on such predictions.

2. Materials and Methods

2.1. Dataset for LSTM

The data utilized for the present study were obtained from the experimental programs performed in the laboratories. The experimental program utilizes the Ground Granulated Blast Furnace Slag (GGBFS), different alkali-activator proportions (i.e., NaOH and sodium silicate with 5%, 6%, and 7%), Fine Aggregates (FA), and Coarse Aggregates (CA), shown in Figure 1. The AAC was produced by mixing the GGBFS and aggregates with NaOH and sodium silicate solution. Before utilizing the materials, the physical property test is important.

Fig. 1. Materials used in the study

The physical properties of GGBFS, FA, and CA are listed in Table 1. The specific mix design of the geopolymer, as detailed in Table 2, is central to the present study. It outlines the precise proportions and components used to create the geopolymer mixture. This includes the type and quantity of raw materials, such as GGBFS, CA, FA, and activators like sodium hydroxide and sodium silicate. The casting of samples was done for compressive strength (cubes), split tensile test (cylinders), and flexural strength (prisms) (Figure 2a). The curing of samples was carried out in curing tanks. The testing program was performed after a maturity period of 28 days. The tests were performed at ambient temperature (27 ^{o}C) and elevated temperature of 100 ^{o}C, 200 ^{o}C, 300 ^{o}C, 400 ^{o}C, 500 ^{o}C, 600 ^{o}C, 700 ^{o}C, and 800 ^{o}C.

The samples were exposed to elevated temperatures using the muffle furnace (Figures 2b and 2c). The compressive (Figure 3a), flexural (Figure 3b), and split tensile strength (Figure 3c) test was performed to collect the data for the present study. The test setup for the experimental programs is shown in Figure 3.

Table 1. Physical characteristics of GGBFS, FA, and CA

Physical properties	GGBFS	FA	CA
Density (kN/m^3)	----------	13.74	15.24
Specific gravity	2.86	2.50	2.75
Fineness	----------	2.85	6.03
Specific surface (cm^2/g)	4235	----------	----------
Water absorptions (%)	----------	1.22	0.43
Bulking (%)	----------	4	----------
Grading	----------	II-zone	----------

Table 2. Mix design used for the experimental study

GGBFS (kg/m^3)	FA (kg/m^3)	CA (kg/m^3)	Alkali sol^n. (%)	w/c ratio
356	1121.4	694.2	5,6, 7	0.42, 0.45, 0.48

(a) **(b)** **(c)**

Fig. 2. Photographs of experimental programs: a) Casted samples; b) Muffle furnace; and c) Samples in muffle furnace

(a) **(b)** **(c)**

Fig. 3. Test programs setups: a) Compressive strength test; b) Flexural strength test; and c) Split tensile test

2.2. Methodology

LSTM is a type of RNN designed to address the challenges posed by vanishing and exploding gradients in traditional RNNs. The vanishing gradient problem arises when training RNNs on long sequences, causing the gradients to become extremely small and hindering the learning of long-term dependencies. LSTM introduces a specialized memory cell to capture and retain information over extended periods, mitigating these gradient-related issues. LSTM's fundamental innovation lies in its architecture, featuring a memory cell with three gates: an input gate, a forget gate, and an output gate. These gates regulate the flow of information into, out of, and within the memory cell, allowing the network to remember or forget information selectively.

This mechanism enables LSTMs to maintain context over extended sequences, making them particularly adept at learning and exploiting long-term dependencies in data (Figure 4). The ability of LSTMs to memorize information for prolonged durations positions them as powerful tools for processing sequential data, such as time series. Time series data often exhibits dependencies across multiple time steps, and LSTM's capacity to capture and remember these dependencies makes them well-suited for tasks like time series analysis. By retaining crucial information over extended periods, LSTMs excel in recognizing patterns, trends, and relationships within sequential data, contributing to more accurate modeling and prediction. In this study, data obtained from experimental programs play a crucial role, strategically employed in a 70-30 ratio. For each type of test, 57 data sets have been used.

This distribution serves a dual purpose in training and evaluating the machine learning model for predicting the mechanical properties of AAC under consideration. 70% of the collected data is dedicated to training the model, allowing it to learn and discern patterns inherent in the dataset. Through this training process, the model grasps the underlying relationships between various factors and the mechanical properties of AAC at elevated temperatures.

The remaining 30% of the data is reserved for testing the model's efficiency and generalization capabilities. This evaluation ensures the model's reliability and applicability beyond the training dataset. In essence, the 70-30 data split strategy ensures a robust and validated machine learning model that can accurately predict the mechanical properties of AAC under elevated temperature conditions.

Splitting the dataset for evaluation is essential to objectively measure the model's predictive performance before applying the data in ML. This step involves calculating various statistical measures such as the mean, standard deviation, minimum, and maximum values. By doing so, one can comprehensively understand the dataset's attributes. Analyzing these statistics helps identify trends, patterns, and outliers, crucial for making informed decisions during the model development phase. This preliminary analysis ensures that any anomalies or inconsistencies in the data are detected early, facilitating the creation of a more robust and accurate model. The findings from this statistical evaluation are then organized and presented in Table 3.

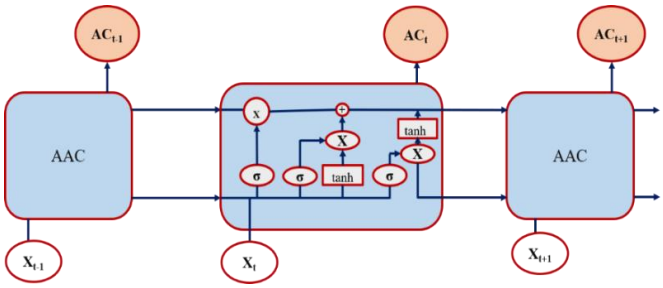

Fig. 4. LSTM architecture

3. Results and Discussion

The present study centers on forecasting the mechanical properties of AAC under elevated temperatures, employing LSTM networks for this purpose. This section focuses on creating and validating predictive LSTM models specifically designed to predict the concrete strength of AAC at elevated temperatures.

3.1. Compressive Strength Prediction and Error Analysis

The initial step involves developing a predictive model for the Compressive Strength (CS) of AAC using LSTM. The compressive strength predictive model undergoes two crucial phases: training and testing. During training, the LSTM model learns from a dataset containing information on AAC's mechanical properties under various temperature conditions. The reported coefficient of determination (R^2) values of 0.9838 and 0.9114 during training and testing signify a strong correlation between the predicted and actual compressive strength values, indicating that the model successfully captures the underlying patterns and relationships in the training data (Figures 5a and 5b).

The Hyper parameters are used in the LSTM model for compressive strength prediction, typically employing 1 to 3 layers, each consisting of 50 to 300 units per layer. The sequence length, which defines the number of time steps or input features considered simultaneously, ranged between 10 to 50. A learning rate between 0.001 to 0.01 was selected to optimize the gradient descent algorithm during training, ensuring efficient convergence and model stability. Batch sizes varied from 16 to 64, influencing how many samples were processed before updating model weights, while dropout rates, set between 0.1 to 0.5, regulated the regularization of network connections to prevent overfitting. Activation functions such as tanh were chosen to introduce non-linearity into the model, effectively capturing complex relationships within the AAC dataset. The error analysis of a compressive strength prediction model involves assessing its accuracy by comparing the predicted strength with actual experimental data.

Table 3. The statical analysis results of the parameters used in the analysis

	GGBFS	CA	FA	w/c ratio	Alkali (%)	Temperature (°C)	CS	TS	FS
Count	81	81	81	81	81	81	81	81	81
Mean	356	1121.4	694.2	0.45	6	403	21.75	2.23	2.34
Std	0	0.0	0.0	0.03	0.8	255.3	10.52	1.52	1.75
Min	356	1121.4	694.2	0.42	5	27	2.86	0.39	0.19
25%	356	1121.4	694.2	0.42	5	200	11.02	0.98	0.8
50%	356	1121.4	694.2	0.45	6	400	25.01	1.92	1.84
75%	356	1121.4	694.2	0.48	7	600	29.72	2.83	3.74
Max	356	1121.4	694.2	0.48	7	800	40.37	6.11	6.48

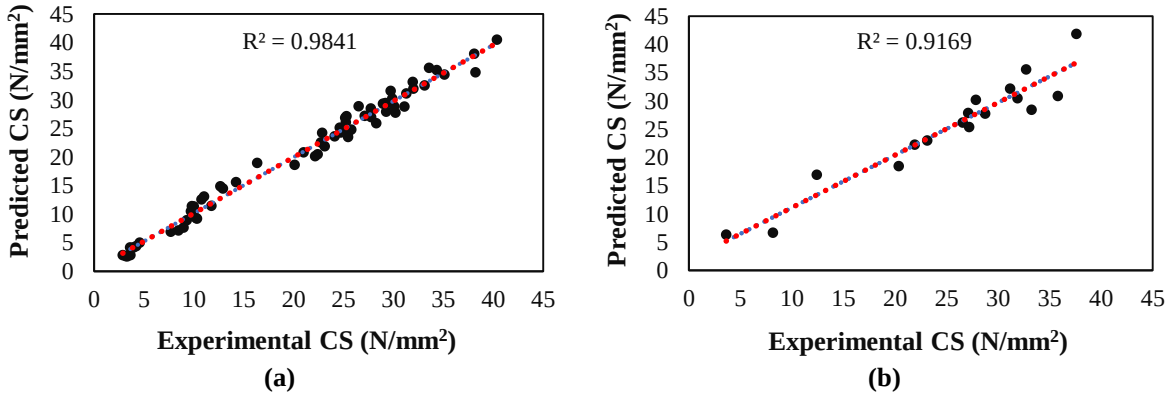

Fig. 5. Compressive strength prediction for: a) Training; and b) Testing

In Figures 6a and 6b, the study focuses on the training and testing phases, visually representing the errors encountered. The term "error" refers to the disparity between predicted values from the model and the actual experimental results. The figures indicate minimal deviation between predicted and experimental values in both phases. This suggests that the model's predictions for the compressive strength of AAC under elevated temperatures closely align with the values obtained through experimentation. The small discrepancies observed in the error study imply a high degree of accuracy in the model's ability to forecast compressive strength under these conditions.

3.2. Flexural Strength Prediction and Error Analysis

The Flexural Strength (FS) data acquired from laboratory experiments is the foundation for training and evaluating a predictive model. The model's efficacy is assessed using the performance parameter R^2, which gauges the goodness of fit between the predicted values and the actual experimental results. The R^2 value of 0.9965 (Figure 7a) for the training phase suggests an extremely robust fit during the model's learning process, affirming its capacity to reproduce the observed flexural strength within the laboratory setting accurately. The slightly lower R^2 value of 0.98611 (Figure 7b) for the testing phase indicates a slightly reduced but impressive performance when applied to new, unseen data. Verifying predicted flexural strength involves a comparative analysis between the model's predictions and actual experimental data.

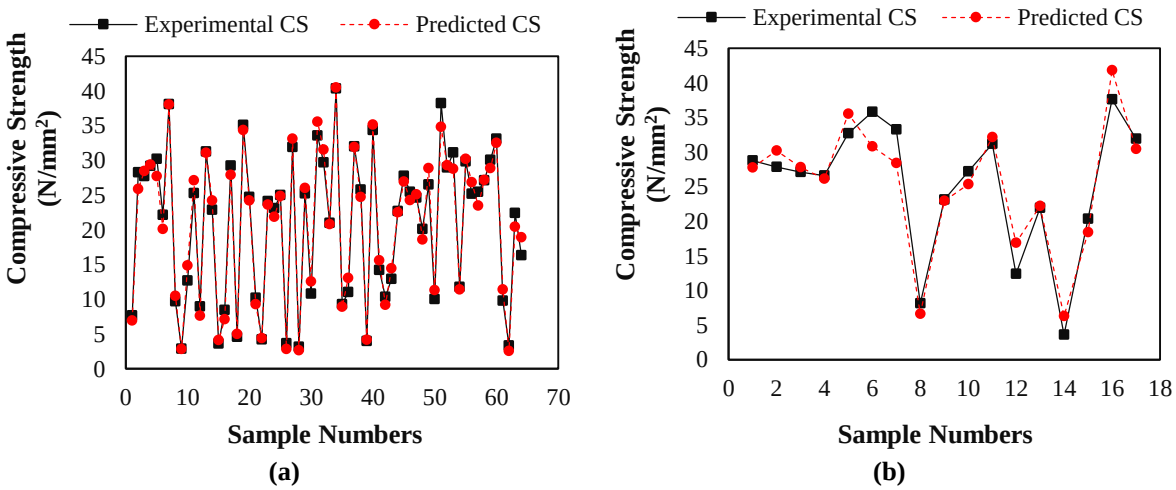

Fig. 6. Compressive strength Error for: a) Training; and b) Testing

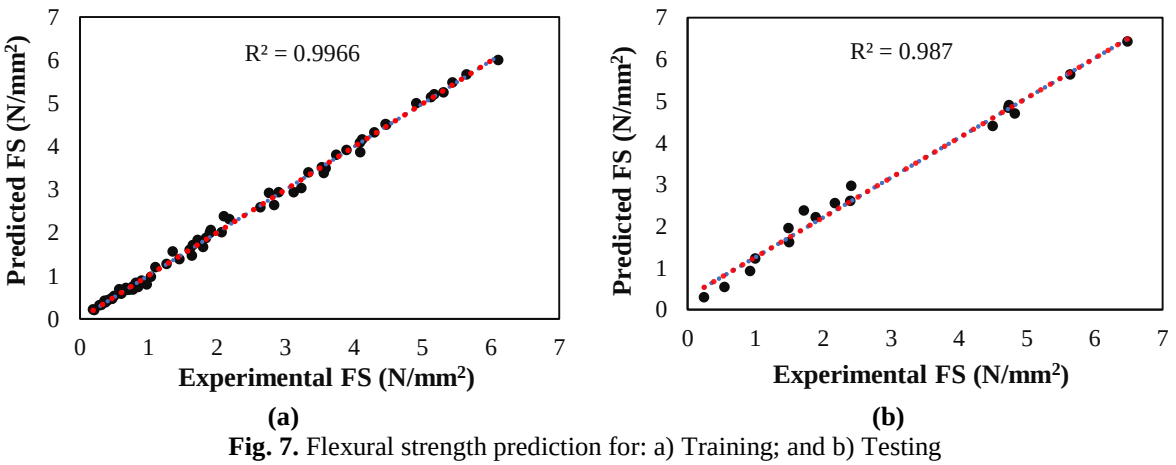

Fig. 7. Flexural strength prediction for: a) Training; and b) Testing

Figures 8a and 8b illustrate this investigation for the training and testing phases. These figures are a crucial validation step for the predictive model's accuracy, particularly under elevated temperature conditions for AAC. The minimal difference observed between the predicted and experimental values in both phases indicates high accuracy and reliability in the model's predictions for the flexural strength of AAC under elevated temperature conditions. This suggests that the model effectively captures and reproduces the complex relationships within the data, demonstrating its ability to generalize well to new, unseen instances.

The hyperparameters are used for flexural strength prediction; LSTM architectures span 1 to 4 layers with 50 to 400 units per layer. The sequence length and learning rate mirrored those used for compressive strength prediction, adapting to the specific dynamics of flexural strength data. Batch sizes and dropout rates were adjusted similarly to compressive strength models to balance computational efficiency and model robustness. Activation functions like ReLU or tanh were preferred here, catering to the nature of flexural strength data, and enhancing the model's ability to capture nonlinear dependencies.

3.3. Split Tensile Strength Prediction and Error Analysis

Developing a predictive model for the Split Tensile Strength (STS) of AAC mirrors the approach taken for compressive and flexural strength prediction models. The process involves initial training of the model followed by testing with experimental data, divided into 70% for training and 30% for testing. The model's performance is evaluated using the performance coefficient, R^2. In the training phase, the obtained R^2 value of 0.9743 (Figure 9a) indicates a strong correlation between the model's predictions and the actual split tensile strength data used for training.

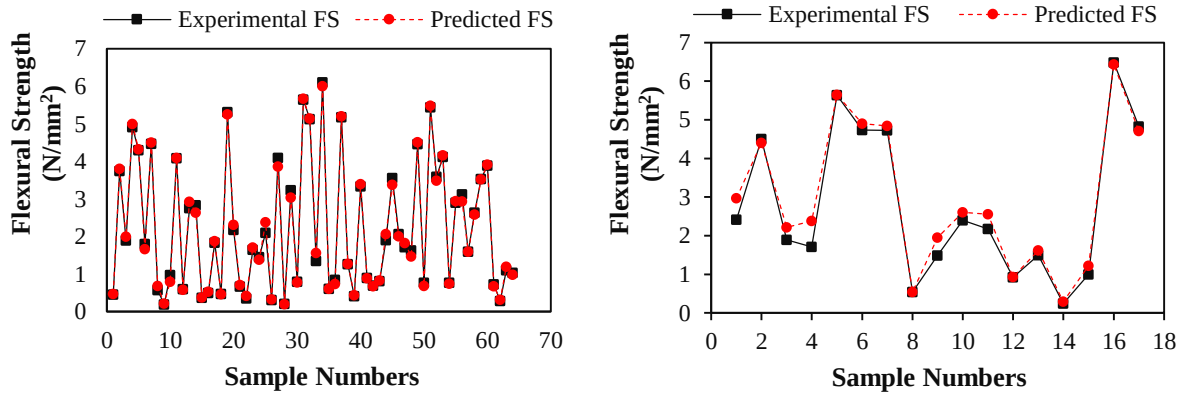

Fig. 8. Flexural strength error for: a) Training; and b) Testing

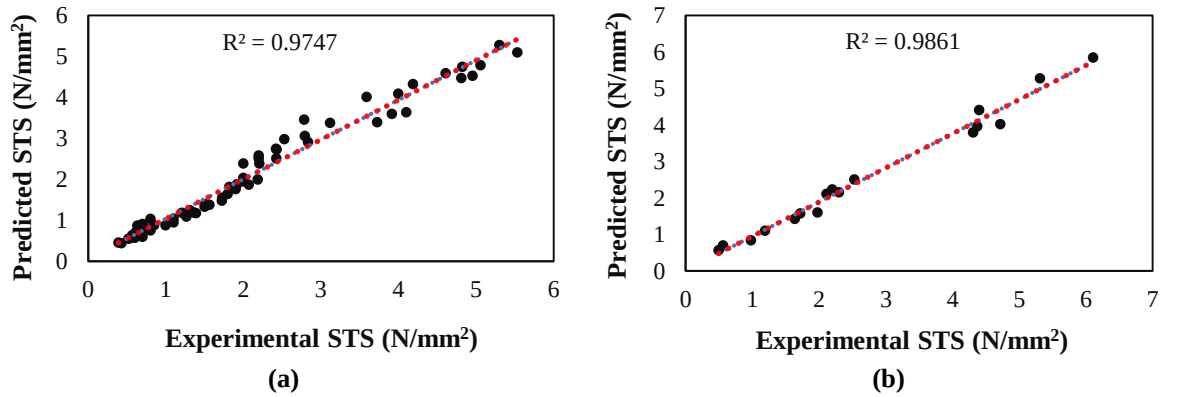

Fig. 9. Split tensile strength prediction for: a) Training; and b) Testing

This high R^2 value suggests that the model effectively captures the underlying patterns and relationships in the training data. Similarly, in the testing phase, the R^2 value of 0.9852 (Figure 9b) signifies a robust performance when applied to new, unseen data. This indicates the model's ability to generalize well beyond the training dataset, providing accurate predictions for split tensile strength under conditions not encountered during the training phase. In predicting split tensile strength, LSTM networks typically mirrored the configurations used for compressive strength, with 1 to 3 layers and 50 to 300 units per layer. Sequence lengths, learning rates, batch sizes, and dropout rates aligned closely with those used in compressive and flexural strength models, ensuring consistency in training approaches across different mechanical properties.

Activation functions such as tanh or sigmoid were selected to effectively model the split tensile strength data, aiming to optimize predictive accuracy under varying thermal conditions. The error analysis of the split tensile strength prediction model follows a methodology like that employed for the compressive and flexural strength prediction models.

In Figures 10a and 10b, a graphical representation compares predicted and experimental split tensile strength values for the training and testing phases. This visualization enables a comprehensive examination of the model's accuracy. The outcome of the error analysis reveals a close similarity between predicted and experimental strength values. The minimal deviation observed in the training and testing phases suggests that the model performs exceptionally well. The closely aligned predicted and experimental values indicate that the model accurately captures the intricate relationships within the split tensile strength data.

Table 3 serves as a comprehensive summary of the model's performance in predicting the mechanical properties of AAC. The assessment employs three optimizer evaluation functions: R^2, Root Mean Square Error (RMSE), and Mean Absolute Error (MAE) . These metrics are crucial in gauging the developed model's accuracy and reliability in predicting AAC's mechanical properties. The results presented in Table 4, indicate that, across all models, there is an observable trend of superior performance. This implies that the LSTM models consistently demonstrate effectiveness in capturing and predicting the mechanical characteristics of AAC.

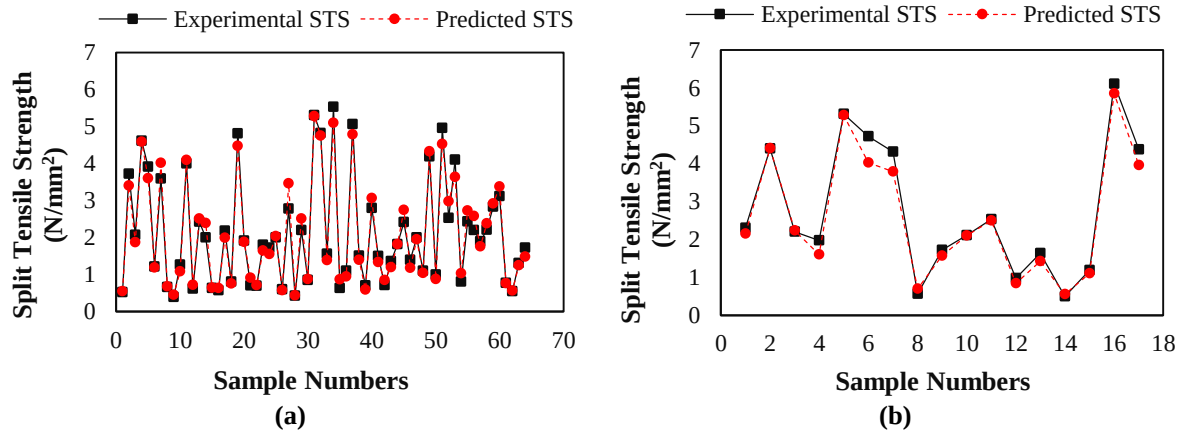

Fig. 10. Split tensile strength Error for: a) Training; and b) Testing

Table 4. Assessing the performance metrics of LSTM networks using various coefficients

Coefficient	Compressive strength		Flexural strength		Split tensile strength	
	Training	Testing	Training	Testing	Training	Testing
R^2	0.9838	0.9134	0.9965	0.9861	0.9743	0.9852
RMSE	1.3323	2.6696	0.098	0.2865	0.2663	0.2727
MAE	1.0784	2.1625	0.0727	0.2094	0.1733	0.1941

The use of R^2, RMSE, and MAE as evaluation criteria collectively reinforces the robustness of the model, as these metrics provide a holistic assessment of predictive accuracy, error distribution, and absolute prediction deviations.

4. Conclusions

The present study experimentally investigated the mechanical properties of AAC. The present study employed LSTM networks to accurately predict these properties under elevated temperatures. The LSTM models demonstrated strong performance, with R^2 exceeding 0.9 for compressive strength (training: 0.9838, testing: 0.9134), flexural strength (training: 0.9965, testing: 0.9861), and split tensile strength (training: 0.9743, testing: 0.9852). Additionally, low RMSE and MAE values (compressive strength: RMSE 1.3323, MAE 1.0784; flexural strength: RMSE 0.098, MAE 0.0727; split tensile strength: RMSE 0.2663, MAE 0.1733) further confirm the models' accuracy in predicting AAC behaviour under extreme thermal conditions. Further error analysis was conducted for all three properties, affirming the robustness of the LSTM networks in capturing the intricate relationships within AAC datasets. These findings highlight the potential of LSTM models to enhance predictions of material properties essential for structural fire safety assessments and sustainable construction practices.

5. Future Scope

Expanding the present dataset to include a broader spectrum of temperatures exceeding 800 °C holds the potential for refining predictions in more severe thermal environments. Moreover, augmenting the dataset with diverse compositions of alkali activators and supplementary materials like metakaolin or slag could bolster the model's robustness and extend its applicability across various AAC formulations.

Additionally, integrating advanced machine learning techniques such as ensemble or hybrid models that combine LSTM with other algorithms could further elevate prediction accuracy. Beyond predictive prowess, future research could explore optimizing AAC mix designs to achieve specific mechanical properties under diverse environmental conditions. Moreover, validating these predictive models in practical settings, such as in structural fire safety assessments or sustainable construction practices, could substantiate their real-world utility and promote widespread adoption within the construction industry.

6. Declaration

The authors declare that they have not used generative artificial intelligence (AI) or AI-assisted technologies.

7. References

Abhishek, H.S., Prashant, S., Kamath, M.V. and Kumar, M. (2022). "Fresh mechanical and durability properties of alkali-activated fly ash-slag concrete: A review", *Innovative Infrastructure Solutions*, 7, 116, https://doi.org/10.1007/s41062-021-00711-w.

Alrefaei, Y. and Dai, J.G. (2018). "Tensile behavior and microstructure of hybrid fiber ambient cured one-part engineered geopolymer composites", *Construction and Building Materials*, 184, 419-431, https://doi.org/10.1016/j.conbuildmat.2018.07.012.

Bai, J., Wild, S., Ware, J.A. and Sabir, B.B. (2003). "Using neural networks to predict workability of concrete incorporating metakaolin and fly ash", *Advances in Engineering Software*, 34(11-12), 663-669, https://doi.org/10.1016/S0965-9978(03)00102-9.

Chithambaram, S.J., Kumar, S. and Prasad, M.M. (2019). "Thermo-mechanical characteristics of geopolymer mortar", *Construction and Building Materials*, 213, 100-108, https://doi.org/10.1016/j.conbuildmat.2019.04.051.

Criado, M., Fernández-Jiménez, A. and Palomo, A. (2010). "Alkali activation of fly ash, part III: Effect of curing conditions on reaction and its graphical description", *Fuel*, 89(11), 3185-3192, https://doi.org/10.1016/j.fuel.2010.03.051.

Dueramae, S., Tangchirapat, W., Chindaprasirt, P., Jaturapitakkul, C. and Sukontasukkul, P. (2020). "Autogenous and drying shrinkages of mortars and pore structure of pastes made with activated binder of calcium carbide residue and fly ash", *Construction and Building Materials*, 230,

116962, https://doi.org/10.1016/j.conbuildmat.2019.116962.

Duxson, P., Fernández-Jiménez, A., Provis, J.L., Lukey, G.C., Palomo, A. and van Deventer, J.S.J. (2007). "Geopolymer technology: the current state of the art", *Journal of Materials Science*, 42, 2917-2933, https://doi.org/10.1007/s10853-006-0637-z.

Fernandez-Jimenez, A.M., Palomo, A. and Lopez-Hombrados, C. (2006). "Engineering properties of alkali-activated fly ash concrete", *ACI Materials Journal*, 103(2), 106-112, https://doi.org/10.14359/15261.

Garcia-Lodeiro, I., Palomo, A., Fernández-Jiménez, A. and Macphee, D.E. (2011). "Compatibility studies between NASH and CASH gels, Study in the ternary diagram Na_2O-CaO-Al_2Oo_3-SiO_2-H_2O", *Cement and Concrete Research*, 41(9), 923-931, https://doi.org/10.1016/j.cemconres.2011.05.006.

Gogineni, A., Panday, I.K., Kumar, P. and Paswan, R.K. (2024a). "Predicting compressive strength of concrete with fly ash and admixture using XGBoost: A comparative study of machine learning algorithms", *Asian Journal of Civil Engineering*, 25(1), 685-698, https://doi.org/10.1007/s42107-023-00804-0.

Gogineni, A., Panday, I.K., Kumar, P. and Paswan, R.K. (2024b). "Predictive modelling of concrete compressive strength incorporating GGBS and alkali using a machine-learning approach", *Asian Journal of Civil Engineering*, 25(1), 699-709, https://doi.org/10.1007/s42107-023-00805-z.

Gogineni, A., Sharma, S., Roy, S., & Kumar, P. (2026). "Long-term drought analysis and forecasting using hybrid wavelet Denoise random forest models with SPI, Z-score, and China Z-index", *Arabian Journal for Science and Engineering*, 51(4), 5097-5125, https://doi.org/10.1007/s13369-025-10575-2

Huynh, A.T., Nguyen, Q.D., Xuan, Q.L., Magee, B., Chung, T., Tran, K.T. and Nguyen, K.T. (2020). "A machine learning-assisted numerical predictor for compressive strength of geopolymer concrete based on experimental data and sensitivity analysis", *Applied Sciences*, 10(21), 7726, https://doi.org/10.3390/app10217726.

Jithendra, C. and Elavenil, S. (2020). "Influences of parameters on slump flow and compressive strength properties of aluminosilicate-based flowable geopolymer concrete using Taguchi method", *Silicon*, 12(3), 595-602, https://doi.org/10.1007/s12633-019-00166-w.

Khosravani, M.R., Nasiri, S., Anders, D. and Weinberg, K. (2019). "Prediction of dynamic properties of ultra-high-performance concrete by an artificial intelligence approach", *Advances in Engineering Software*, 127, 51-58, https://doi.org/10.1016/j.advengsoft.2018.10.002.

Kim, J.I. and Kim, D.K. (2002). "Application of neural networks for estimation of concrete strength", *KSCE Journal of Civil Engineering*, 6(4), 429-438, https://doi.org/10.1007/BF02841997.

Kovalchuk, G., Fernández-Jiménez, A. and Palomo, A. (2007). "Alkali-activated fly ash: effect of thermal curing conditions on mechanical and microstructural development - Part II", *Fuel*, 86(3), 315-322, https://doi.org/10.1016/j.fuel.2006.07.010.

Kumar, P. and Pratap, B. (2024). "Feature engineering for predicting compressive strength of high-strength concrete with machine learning models", *Asian Journal of Civil Engineering*, 25(1), 723-736, https://doi.org/10.1007/s42107-023-00807-x.

Kumar, P., Gogineni, A. and Upadhyay, R. (2024). "Mechanical performance of fiber-reinforced concrete incorporating rice husk ash and recycled aggregates", *Journal of Building Pathology and Rehabilitation*, 9, 144, https://doi.org/10.1007/s41024-024-00500-9.

Kumar, P., Pratap, B., Sharma, S. and Kumar, I. (2024). "Compressive strength prediction of fly ash and blast furnace slag-based geopolymer concrete using convolutional neural network", *Asian Journal of Civil Engineering*, 25(2), 1561-1569, https://doi.org/10.1007/s42107-023-00861-5.

Kumar, P., Sharma, S. and Pratap, B. (2025a). "Prediction of compressive strength of geopolymer fiber reinforced concrete using machine learning", *Civil Engineering Infrastructures Journal*, 58(1), 173-182, https://doi.org/10.22059/ceij.2024.364871.1956.

Kumar, P., Gogineni, A., Kumar, A. and Modi, P. (2025b). "A comparative analysis of machine learning algorithms for predicting fundamental periods in reinforced concrete frame buildings", *Iranian Journal of Science and Technology, Transactions of Civil Engineering*, 49, 2257-2276, https://doi.org/10.1007/s40996-024-01560-0.

Lee, S., Park, S., Kim, T., Lieu, Q.X. and Lee, J. (2021). "Damage quantification in truss structures by limited sensor-based surrogate model", *Applied Acoustics*, 172, 107547, https://doi.org/10.1016/j.apacoust.2020.107547.

Lieu, Q.X., Nguyen, K.T., Dang, K.D., Lee, S., Kang, J. and Lee, J. (2022). "An adaptive surrogate model to structural reliability analysis using deep neural network", *Expert Systems with Applications*, 189, 116104, https://doi.org/10.1016/j.eswa.2021.116104.

Liu, J.C. and Zhang, Z. (2020). "Neural network models to predict explosive spalling of PP fiber

reinforced concrete under heating", *Journal of Building Engineering*, 32, 101472, https://doi.org/10.1016/j.jobe.2020.101472.

Mishra, P., Srivastav, A., Kumar, P. and Sahu, S.K. (2024). "Comprehensive review of seismic performance assessment for skew-reinforced concrete box-girder bridges", *Asian Journal of Civil Engineering*, 25, 3285-3299, https://doi.org/10.1007/s42107-023-00979-6.

Mostafaei, H., Behnamfar, F. and Alembagheri, M. (2022). "Reliability and sensitivity analysis of wedge stability in the abutments of an arch dam using artificial neural network", *Earthquake Engineering and Engineering Vibration*, 21(4), 1019-1033, https://doi.org/10.1007/s11803-022-2133-0.

Mostafaei, H., Bahmani, H., Mostofinejad, D. and Wu, C. (2023). "A novel development of HPC without cement: mechanical properties and sustainability evaluation", *Journal of Building Engineering*, 76, 107262, https://doi.org/10.1016/j.jobe.2023.107262.

Nagajothi, S. and Elavenil, S. (2020). "Influence of aluminosilicate for the prediction of mechanical properties of geopolymer concrete–artificial neural network", *Silicon*, 12(5), 1011-1021, https://doi.org/10.1007/s12633-019-00203-8.

Nagaraj, Y., Jagannatha, N., Sathisha, N. and Niranjana, S.J. (2021). "Prediction of material removal rate and surface roughness in hot air-assisted hybrid machining on soda-lime-silica glass using regression analysis and artificial neural network", *Silicon*, 13(11), 4163-4175, https://doi.org/10.1007/s12633-020-00729-2.

Namarak, C., Tangchirapat, W. and Jaturapitakkul, C. (2018). "Bar-concrete bond in mixes containing calcium carbide residue, fly ash and recycled concrete aggregate", *Cement and Concrete Composites*, 89, 31-40, https://doi.org/10.1016/j.cemconcomp.2018.02.017.

Neville, A.M. (1995). *Properties of concrete*, Pearson Education India, https://scirp.org/reference/referencespapers?referenceid=2542196.

Paswan, R.K., Gogineni, A., Sharma, S. and Kumar, P. (2024). "Predicting split tensile strength in portland and geopolymer concretes using machine learning algorithms: a comparative study", *Journal of Building Pathology and Rehabilitation*, 9, 129, https://doi.org/10.1007/s41024-024-00485-5.

Patel, Y.J. and Shah, N. (2018). "Enhancement of the properties of ground granulated blast furnace slag-based self-compacting geopolymer concrete by incorporating rice husk ash", *Construction and Building Materials*, 171, 654-662, https://doi.org/10.1016/j.conbuildmat.2018.03.166.

Pratap, B., Kumar, P., Shubham, K. and Chaudhary, N. (2024). "Soft computing-based investigation of mechanical properties of concrete using ready-mix concrete waste water as partial replacement of mixing portable water", *Asian Journal of Civil Engineering*, 25(2), 1255-1266, https://doi.org/10.1007/s42107-023-00841-9.

Pratap, B. and Kumar, P. (2024). "Effect of the elevated temperature on the mechanical properties of geopolymer concrete using fly ash and ground granulated blast slag", *Journal of Structural Fire Engineering*, 15(3), 409-425, https://doi.org/10.1108/JSFE-06-2023-0028.

Reddy, M.Y. and Harihanandh, M. (2023). "Experimental studies on strength and durability of alkali-activated slag and coal bottom ash based geopolymer concrete", *Materials Today: Proceedings*, https://doi.org/10.1016/j.matpr.2023.03.644.

Shah, S.F.A., Chen, B., Oderji, S.Y., Haque, M.A. and Ahmad, M.R. (2020). "Comparative study on the effect of fiber type and content on the performance of one-part alkali-activated mortar", *Construction and Building Materials*, 243, 118221, https://doi.org/10.1016/j.conbuildmat.2020.118221.

Sharma, S., Kumar, A., Bano, S. and Kumar, P. (2024). "Soft computing techniques for analysing the mechanical properties of egg shell powder-based concrete", *Advances in Civil and Architectural Engineering*, 15(28), 119-132, https://doi.org/10.13167/2024.28.9.

Singh, P., Prasad, B. and Kumar, V. (2024). "Influence of elevated temperature on compressive strength of LD slag aggregate concrete", *Journal of Structural Fire Engineering*, 15(1), 76-90, https://doi.org/10.1108/JSFE-08-2022-0028.

Xu, H., Gong, W., Syltebo, L., Izzo, K., Lutze, W. and Pegg, I.L. (2014). "Effect of blast furnace slag grades on fly ash based geopolymer waste forms", *Fuel*, 133, 332-340, https://doi.org/10.1016/j.fuel.2014.05.018.

Yang, D.S., Park, S.K. and Lee, J.H. (2003). "A prediction on mix proportion factor and strength of concrete using neural network", *KSCE Journal of Civil Engineering*, 7(5), 525-536, https://doi.org/10.1007/BF02838318.

Zakka, W.P., Lim, N.H.A.S. and Khun, M.C. (2021). "A scientometric review of geopolymer concrete", *Journal of Cleaner Production*, 280, 124353, https://doi.org/10.1016/j.jclepro.2020.124353.

Zurada, J. (1992). *Introduction to artificial neural systems*, West Publishing Company, https://scirp.org/reference/referencespapers?referenceid=1170384.